

Sol-gel synthesis and the investigation of the properties of nanocrystalline holmium orthoferrite

A. T. Nguyen¹, H. L. T. Tran¹, Ph. U. T. Nguyen¹, I. Ya. Mittova², V. O. Mittova³,
E. L. Viryutina², V. H. Nguyen⁴, X. V. Bui⁵, T. L. Nguyen^{6,7}

¹Ho Chi Minh City University of Education, Ho Chi Minh City 700000, Vietnam

²Voronezh State University, Universitetskaya pl. 1, Voronezh, 394018, Russia

³Burdenko Voronezh State Medical University, Voronezh, 394036, Russia

⁴Dong Thap University, Cao Lanh City 81000, Vietnam

⁵Sai Gon University, Ho Chi Minh City, 700000, Vietnam

⁶Institute of Fundamental and Applied Sciences, Duy Tan University, Ho Chi Minh City, 700000, Vietnam

⁷Faculty of Environmental and Chemical Engineering, Duy Tan University, Da Nang, 550000, Vietnam

tienna@hcmue.edu.vn, tran.hongle86@gmail.com, nguyenphuonguyen0110@gmail.com, imittova@mail.ru,
vmittova@mail.ru, viryutina.helena@yandex.ru, nguyenvanhung@dthu.edu.vn,
buixuanvuongsgu@gmail.com, nguyentuanloi@duytan.edu.vn

DOI 10.17586/2220-8054-2020-11-6-698-704

Holmium orthoferrite nanocrystals (HoFeO₃) were synthesized from an aqueous solution by the sol-gel method, using polyvinyl alcohol as a stabilizer and annealing at temperatures of 650, 750, and 850 °C for an hour. According to the results of the performed analyses, it was found that with an increase in the annealing temperature, the average size of HoFeO₃ crystallites increases from 24 to 30 nm. The magnetic characteristics of the samples were measured and it was shown that holmium orthoferrite is a paramagnet with a low coercive force. The band gap of nanocrystalline holmium ferrite is determined.

Keywords: nanoparticles, holmium orthoferrite, sol-gel technique, magnetic properties, optical properties.

Received: 28 August 2020

Revised: 25 September 2020

Final revision: 20 October 2020

1. Introduction

One of the promising areas of materials science is the creation of effective magnetoelectric ferrites using various synthesis methods. Therefore, recently, orthoferrites of rare-earth metals, especially such a promising and still very poorly studied material as holmium ferrite with a perovskite structure were of interest. Nanocrystalline HoFeO₃ is a multiferroic with a potentially unusual combination of electrical, magnetic, and optical properties [1–4]. AFeO₃ samples are interesting due to their magnetic characteristics and application prospects. For example, they can be compatible with biological materials [5], their nanoparticles can be used as small probes [6–9], which would allow registering the cellular processes without affecting their course. In addition, particles of the nanometer size range are used to increase the density of magnetic recording of information [10–12], production of the transformer coils and other electrical devices with high efficiency [10, 13, 14].

Some orthoferrites are widely used in microwave devices due to their low coercive force (H_c), remnantmagnetization (M_r) and high saturation magnetization (M_S), excellent mechanical and chemical stability, rectangular hysteresis loop, etc. [12, 15, 16].

For the synthesis of orthoferrites, the sol-gel method, which allows production of nanopowders with a narrow particle size distribution at relatively low temperatures, is especially important [15, 18]. The presented method allows production of highly dispersed powders, fibers or thin films from solutions at temperatures lower than in the case of traditional solid-phase systems [19–24]. Such materials can be imparted with completely new functional characteristics, completely different from the characteristics of conventional materials by controlling the composition, size, and shape of nanocrystals [14, 25].

One of the promising methods for producing orthoferrites, which allows improving the above parameters, is the solution combustion method. This method can lead to the synthesis of ferrites with small particle and grain sizes, high density and conversion rates, excellent electromagnetic parameters and a homogeneous microstructure [3, 26–30].

Previously, the features of the formation of orthorhombic and hexagonal holmium orthoferrite during heat treatment (625 – 725 °C for 8 hours) of the products of glycine-nitrate combustion were studied [3]. The photocatalytic activity of orthorhombic HoFeO₃ nanocrystals was studied in the process of photoinduced decomposition of methyl

orange in an aqueous solution under irradiation with visible light. Compared to this method, the sol-gel synthesis is simpler and therefore it is often more preferable. In prior research for the synthesis of holmium ferrite from a solution, absolute ethanol was used as the solvent [31]. However, for the production of a sufficiently large number of nanocrystals in large laboratories or research institutes, synthesis from an aqueous solution is more preferable for the following reasons. 1. Profitability. 2. Safety. There is no danger of ignition of vapors. 3. Possibility of changing the characteristics of absolute ethanol under the influence of the external environment.

Analysis of the literature data showed the feasibility of the synthesis of holmium ferrite by the sol-gel method. Based on these data, the goal of this study was the synthesis of HoFeO_3 nanocrystals from an aqueous solution using the sol-gel method with the participation of PVA, to characterize them, to determine their magnetic characteristics and the band gap of the obtained nanocrystals, to compare the achieved results with results of other synthesis methods and properties of analogue materials.

2. Experimental

The starting materials for the synthesis of the target object were the following reagents: iron (III) nitrate nonahydrate $\text{Fe}(\text{NO}_3)_3 \cdot 9\text{H}_2\text{O}$, holmium nitrate pentahydrate $\text{Ho}(\text{NO}_3)_3 \cdot 5\text{H}_2\text{O}$, aqueous ammonia solution $\text{NH}_3 \cdot \text{H}_2\text{O}$ (all – “chemically pure”), PVA – polyvinyl alcohol $[-\text{CH}_2-\text{CH}(\text{OH})-]_n$ (GOST 10779-78), acting as a stabilizer-PVA, and distilled water.

Nanocrystalline holmium ferrite was synthesized from an equimolar mixture of holmium (III) and iron (III) nitrates of chemically pure grade in the presence of polyvinyl alcohol (56672 g/mol, $n = 1288$) in an aqueous solution according to the following procedure.

The mixture of 0.05 mol/L $\text{Fe}(\text{NO}_3)_3$ and $\text{Ho}(\text{NO}_3)_3$ (30 ml) was added to 70 ml of boiling distilled water with stirring on a magnetic stirrer. After the addition of salts, magnetic stirring was continued for another 10 min at a temperature above 90 °C. Then, to 200 ml of a boiling solution containing polyvinyl alcohol, 100 ml of the resulting mixture was slowly added with stirring; the ratio of polyvinyl alcohol – sum of metal ions was 1: 3 by weight [32,33]. Over time, the resulting system became concentrated due to water evaporation and stirring was continued with a glass stirring rod until a yellow-brown powder formed.

Thermogravimetric analysis of the powders was carried out using a TGA-DSC thermal analyzer, LabsysEvo 1600 °C (dry air, high purity, 99.99 %; 10 deg/min). The phase composition of the samples was determined by X-ray phase analysis (XRD, D8-Advance diffractometer) with $\text{CuK}\alpha$ radiation. The obtained diffraction patterns were analyzed using the JCPDS database [34]. Parameters a , b , c and crystal cell volume V were determined from the raw file data using the X'pert High Score Plus 2.2b program.

The size of holmium ferrite crystallites according to X-ray diffraction data was determined based on the analysis of the broadening of three maximum lines using the Scherrer formula [35].

The main method for controlling the size and shape of particles was electron microscopy: high-voltage transmission (TEM; JEM-1400) and scanning microscopy (SEM, S-4800).

The elemental composition of the product was monitored by local X-ray spectral microscopy (EDX, Horiba H-7593).

For measurement of the magnetic properties (specific magnetisation and coercive force, excess magnetisation), a VSM Microsene EV11 magnetometer with a vibrating sample was used.

3. Results and discussions

A comprehensive thermal analysis of a holmium ferrite sample obtained by the sol-gel method in the presence of polyvinyl alcohol (Fig. 1a) showed that the weight loss of the sample was 60.47 wt%, which is explained by the evaporation of water and the decomposition of organometallic compounds between Ho^{3+} , Fe^{3+} cations and polyvinyl alcohol, as well as the decomposition of nitrates. A similar situation was observed for lanthanum orthoferrite in the study [20]. A fast and regular weight loss was observed in the range from 50 to ~ 400 °C, and at a higher temperature the sample weight decreased more slowly (about 5.6 %). The processes of decomposition-heating of organometallic compounds under the action of atmospheric oxygen and oxygen formed during the decomposition of nitrates, with the formation of holmium (III) and iron (III) oxides, are accompanied by a number of exothermic effects at 162.21, 216.27, 339.52, 581.69 and 652.36 °C; this can be used for the production of HoFeO_3 nanoparticles by the method of gel combustion as described, for example, in studies [20, 32, 33]. The endothermic effect at 90.82 °C was due to the evaporation of water contained in the sample due to its storage in air.

XRD results show that holmium ferrite samples (Fig. 2) after annealing at 650, 750, and 850 °C for 60 min are single-phase products, all peaks correspond to the reference diffractogram of HoFeO_3 with an orthorhombic structure (map number 046-0115) [34]. With an increase in the annealing temperature from 650 to 750 °C, the intensity of

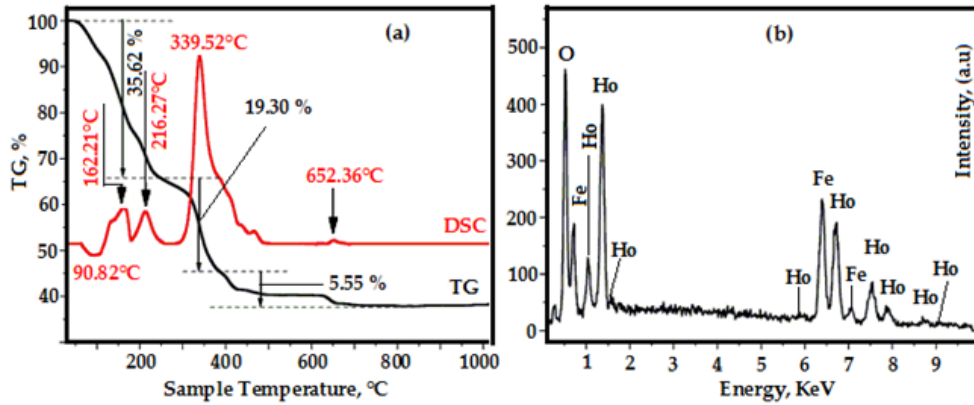


FIG. 1. TGA/DSC curves of the powders prepared by sol-gel technique using PVA (a) and Energy-Dispersive X-ray spectroscopy (EDX) of HoFeO_3 nanoparticles annealed at $750\text{ }^\circ\text{C}$ for 1 h (b)

crystallization of holmium ferrite samples increases, and after annealing the samples in the range $750 - 850\text{ }^\circ\text{C}$, it did not change. According to the results of local X-ray spectral microscopy, the composition of HoFeO_3 after annealing at $750\text{ }^\circ\text{C}$ for 1 h consisted of only three elements – Ho, Fe, and O, i.e. impurity components were not revealed (Fig. 1b). The atomic ratio $\text{Ho}:\text{Fe} = 1:1.01$, which, within the within the measurement accuracy corresponds to their specified nominal composition.

The broadening of X-ray diffraction lines was used to determine the average size of crystallites (regions of coherent scattering) by the Scherrer formula [35]; the results are presented in Table 1. Based on these calculations, we can conclude that the crystallite size does not exceed 30 nm for HoFeO_3 . The calculation of the unit cell parameters from the diffractometry data showed that an increase in the annealing temperature led to a slight increase in the unit cell volume (Table 1), which was also observed in studies [36,37]. As shown in the study [36], a reliable estimate of the crystallite size from the broadening of diffraction peaks is possible only in combination with additional structural data, for example, with the results of electron microscopy.

TABLE 1. Unit cell parameters and average size of HoFeO_3 crystals synthesized from an aqueous solution in the presence of PVA after annealing at different temperatures for 60 min

$t, \text{ }^\circ\text{C}$	$d, \text{ nm}$	$a, \text{ \AA}$	$b, \text{ \AA}$	$c, \text{ \AA}$	$V, \text{ \AA}^3$
650	24	5.2819	5.5801	7.6151	224.444
750	28	5.2824	5.5846	7.6085	224.451
850	30	5.2825	5.5785	7.6239	224.664

SEM, TEM images, and a histogram of the particle size distribution of HoFeO_3 nanopowders synthesized by the sol-gel method from an aqueous solution in the presence of PVA after annealing at $750\text{ }^\circ\text{C}$ for 60 min are shown in Fig. 3. SEM and TEM images showed that the holmium ferrite particles have different shapes: approximately round with a weakly expressed faceting and oval. The diameter of most crystallites (about 80 % of the number of particles) of the presented orthoferrite was in the range of 31 – 40 nm (TEM). In addition, some particles exhibited a shape characteristic of agglomerates, which complicated accurate determination of the size of crystallites and led to a wide distribution of nanoparticles by size.

The process of formation of agglomerates can be caused by the intergrowth of crystallites, including oriented intergrowth, in the process of nucleation and growth of nuclei, as was shown, for example, in studies [38–40] as well as the sintering of nanoparticles during annealing.

Differences in the values of the average diameter according to the Scherrer formula and according to the SEM and TEM data were due to the peculiarities of the methods: the first method allows the determination of the average crystal size in the entire sample, and electron microscopy provides information on a small sample of particles, the dispersed composition of which depends on the sample preparation procedure [42]. In addition, it is not always possible to distinguish between a crystallite and a particle consisting of intergrown crystallites from a micrograph.

Absorption spectrum of HoFeO_3 nanoparticles after annealing at $750\text{ }^\circ\text{C}$ for 1 h in UV light showed strong absorption in the region of ultraviolet and visible light ($\sim 300 - 600\text{ nm}$) (Fig. 4a). This is interesting since HoFeO_3

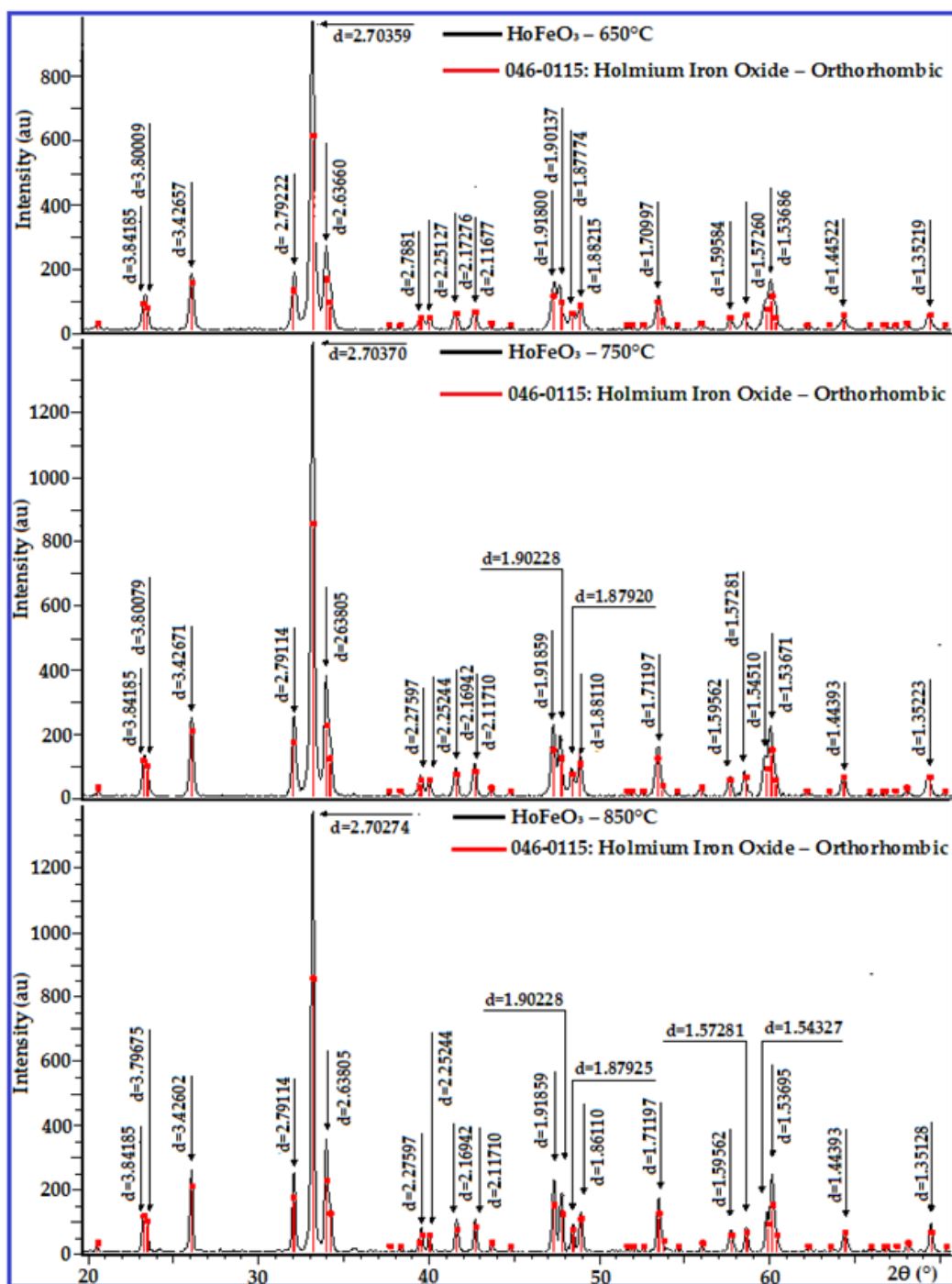


FIG. 2. XRD patterns of HoFeO_3 nanopowders annealed at 650, 750, and 850 °C for 1 h

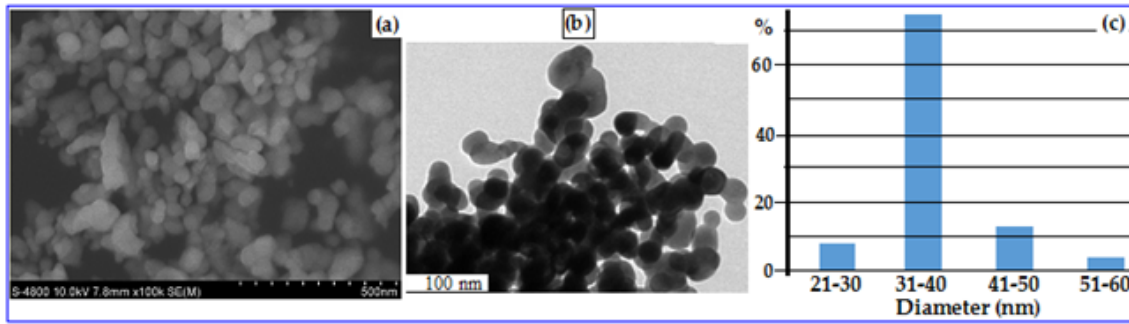


FIG. 3. SEM (a), TEM (b) images and particle size distribution histogram of HoFeO_3 powders annealed at 750°C for 1 h

can be used as a new visible light photocatalyst. Results of determining the photocatalytic activity of the synthesized HoFeO_3 nanocrystals are shown in Fig. 4a. The energy of direct transitions for the band gap was determined by fitting the absorption data to the direct transition, and is presented in the study [36]. As a consequence, the band gap of HoFeO_3 nanoparticles is ~ 1.80 eV (Fig. 4b). Such a small band gap is interesting for the potential application of HoFeO_3 in photocatalysis, sensor and electrode materials in solid oxide fuel cells.

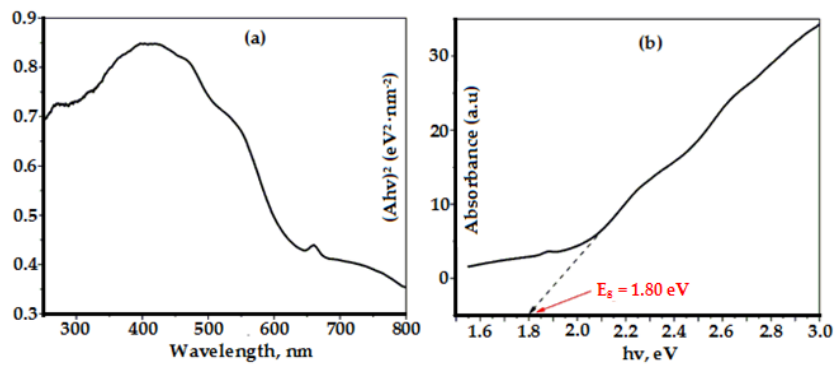


FIG. 4. (a) Room temperature optical absorbance spectrum of the HoFeO_3 sample annealed at 750°C , (b) Plot of $(Ah\nu)^2$ as a function of photon energy for HoFeO_3 nanoparticles

Results of determining the field dependences of the magnetization of a holmium ferrite sample annealed at 750°C , measured at 300 K in a field of 5000 Oe, are presented in Fig. 5a. Nanoparticles HoFeO_3 , obtained by the sol-gel method from an aqueous solution in the presence of PVA, are characterised at the selected annealing temperature by low values of remnant magnetization ($M_r = 0.0044$ emu/g) and coercive force ($H_c = 25.14$ Oe), with high value of the specific magnetization ($M_s = 0.73$ emu/g) and a narrow hysteresis loop (Fig. 5b) and they did not reach magnetic saturation in a field of 5000 Oe. Thus, the synthesized object is paramagnetic.

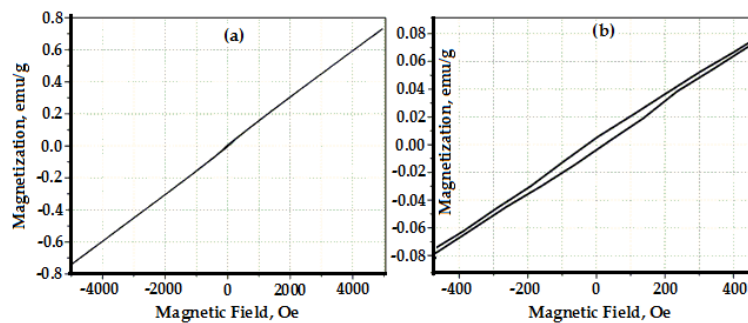


FIG. 5. MH curves at ± 5 kOe measured at RT of the HoFeO_3 sample annealed at 750°C for 1 h

A comparison of the magnetic characteristics of holmium ferrite nanocrystals synthesized in this study from an aqueous solution using PVA is presented in Table 2. As can be seen from the Table 2, these characteristics are not

significantly different from characteristics of the samples synthesised in absolute ethanol [31] and strongly depend on the synthesis method [1, 42]. Interestingly, the synthesized nanocrystalline HoFeO₃ characterized by lower values of H_c, but higher M_s compared with nanoparticles of orthoferrites of other rare earth elements such as YFeO₃, NdFeO₃ obtained by coprecipitation [20, 43], and LaFeO₃ synthesized by the ceramic method [44].

TABLE 2. Magnetic characteristics of HoFeO₃ nanoparticles in this study and from the literature as a comparison

Objects	Coercive force (H _c), Oe	Remnant magnetization (M _r), emu/g	Saturation magnetization (M _s), emu/g
HoFeO ₃ in this study	25.14	4.4·10 ⁻³	0.73
HoFeO ₃ [31]	8.19 ÷ 22.70	1.3·10 ⁻³ ÷ 4.3·10 ⁻³	0.71 ÷ 0.79
HoFeO ₃ [1]	2959	40.8·10 ⁻¹	2.55
HoFeO ₃ [42]	461.13	6.05·10 ⁻²	—
YFeO ₃ [20]	53.36	0.19·10 ⁻³	0.39
NdFeO ₃ [43]	136.76	68.0·10 ⁻²	0.80
LaFeO ₃ [44]	1217.6	5.43·10 ⁻⁴	6.49·10 ⁻³

4. Conclusion

Based on the analysis of the data obtained, it can be concluded that the proposed synthesis procedure leads to the formation of a single-phase nanocrystalline orthoferrite HoFeO₃ with an average crystallite size of about 30 nm. Changing the solvent from absolute ethanol to water with the addition of PVA did not adversely affect the properties of the final product, but it is preferable due to the higher cost effectiveness, safety, and stability of the solvent properties. Synthesized HoFeO₃ nanopowders were characterized by a low band gap, demonstrating the properties of a paramagnetic material, therefore, it is potentially possible to use them not only in photocatalysis, but also as magnetic materials.

Conflict of interests

The authors maintain that they have no conflict of interest with respect to this communication.

Acknowledgements

Nguyen Anh Tien is grateful for the financial support of Ho Chi Minh City University of Education, Ho Chi Minh City, Vietnam, through Grant No. CS.2020.19.21.

References

- [1] Habib Z., Majid K., et al. Influence of Ni substitution at B-site for Fe³⁺ ions on morphological, optical, and magnetic properties of HoFeO₃ ceramics. *Applied Physics A: Materials Science & Processing*, 2016, **122** (5), P. 550–557.
- [2] Shao M., Cao Sh., et al. Single crystal growth, magnetic properties and Schottky anomaly of HoFeO₃ orthoferrite. *Journal of Crystal Growth*, 2011, **318** (1), P. 947–950.
- [3] Kondrashkova I.S., Martinson K.D., Zakharova N.V., Popkov V.I. Synthesis of nanocrystalline HoFeO₃ photocatalyst via heat treatment of products of glycine-nitrate combustion. *Russian Journal of General Chemistry*, 2018, **88** (12), P. 2465–2471.
- [4] Martinson K.D., Kondrashkova I.S., et al. Magnetically recoverable catalyst based on porous nanocrystalline HoFeO₃ for processes of n-hexane conversion. *Advanced Powder Technology*, 2020, **31** (1), P. 402–408.
- [5] Mushtaq M.W., Imran M., et al. Synthesis, structural and biological studies of cobalt ferrite nanoparticles. *Bulgarian Chemical Communications*, 2016, **48** (3), P. 565–570.
- [6] Nikiforov V.N., Filinova E.Yu. Biomedical applications of the magnetic nanoparticles. In book: *Magnetic Nanoparticles*, Wiley-VCH Verlag GmbH & CO. KGaA, Weinheim, 2009, **10**, P. 393–455.
- [7] Gu H., Xu K., Xu C., Xu B. Biofunctional magnetic nanoparticles for protein separation and pathogen detection. *Chemical Communications*, 2006, **37** (9), P. 941–949.
- [8] Albadi Y., Popkov V.I. Dual-modal contrast agent for magnetic resonance imaging based on gadolinium orthoferrite nanoparticles: synthesis, structure and application prospects. *Medicine: theory and practice*, 2019, **4** (S), P. 35–36.
- [9] Albadi Y., Martinson K.D., et al. Synthesis of GdFeO₃ nanoparticles via low-temperature reverse co-precipitation: the effect of strong agglomeration on the magnetic behavior. *Nanosystems: Physics, Chemistry, Mathematics*, 2020, **11** (2), P. 252–259.
- [10] Zhou Zh., Guo L., et al. Hydrothermal synthesis and magnetic properties of multiferroic rare-earth orthoferrites, *Journal of Alloys and Compounds*, 2014, **583**, P. 21–31.

- [11] Park T., Papaefthymiou G.C., et al. Size-dependent magnetic properties of single-crystalline multiferroic BiFeO₃ nanoparticles. *Nano Letters*, 2007, **7** (3), P. 766–772.
- [12] Lomanova N.A., Tomkovich M.V., et al. Magnetic properties of Bi_{1-x}Ca_xFeO_{3-δ} nanocrystals. *Physics of the Solid State*, 2019, **61**, P. 2535–2541.
- [13] Martinson K.D., Ivanov V.A., et al. Facile combustion synthesis of TbFeO₃ nanocrystals with hexagonal and orthorhombic structure. *Nanosystems: Physics, Chemistry, Mathematics*, 2019, **10** (6), P. 694–700.
- [14] Kovalenko A.N., Tugova E.A. Thermodynamics and kinetics of non-autonomous phases formation in nanostructured materials with variable functional properties. *Nanosystems: Physics, Chemistry, Mathematics*, 2018, **9** (5), P. 641–662.
- [15] Popkov V.I., Almjasheva O.V., et al. Magnetic properties of YFeO₃ nanocrystals obtained by different soft-chemical methods. *Journal of Materials Science: Materials in Electronics*, 2017, **28** (10), P. 7163–7170.
- [16] Lomanova N.A., Tomkovich M.V., et al. Thermal and magnetic behavior of BiFeO₃ nanoparticles prepared by glycine-nitrate combustion. *Journal of Nanoparticle Research*, 2018, **20** (2).
- [17] Dmitriev A.V., Vladimirova E.V., et al. Synthesis of hollow spheres of BiFeO₃ from nitrate solutions with tartaric acid: Morphology and magnetic properties. *Journal of Alloys and Compounds*, 2019, **77** (10), P. 586–592.
- [18] Tomina E.V., Kurkin N.A., Mal'tsev S.A. Microwave synthesis of yttrium orthoferrite doped with nickel. *Condensed Matter and Interphases*, 2019, **21** (2), P. 306–312.
- [19] Almjasheva O.V., Krasilin A.A., Gusarov V.V. Formation mechanism of core-shell nanocrystals obtained via dehydration of coprecipitated hydroxides at hydrothermal conditions. *Nanosystems: Physics, Chemistry, Mathematics*, 2018, **9** (4), P. 568–572.
- [20] Nguyen T.A., Almjasheva O.V., et al. Synthesis and magnetic properties of YFeO₃ nanocrystals. *Inorganic Materials*, 2009, **45** (11), P. 1304–1308.
- [21] Popkov V.I., Almyasheva O.V., Schmidt M.P., Gusarov V.V. Formation mechanism of nanocrystalline yttrium orthoferrite under heat treatment of the coprecipitated hydroxides. *Russian Journal of General Chemistry*, 2015, **85** (6), P. 1370–1375.
- [22] Nguyen T.A., Mittova I.Ya., et al. Sol-gel preparation and magnetic properties of nanocrystalline lanthanum ferrite. *Russian Journal of General Chemistry*, 2014, **84** (7), P. 1261–1264.
- [23] Proskurina O.V., Abiev R.S., et al. Formation of nanocrystalline BiFeO₃ during heat treatment of hydroxides co-precipitated in an impinging-jets microreactor. *Chemical Engineering and Processing – Process Intensification*, 2019, **143**, 107598.
- [24] Proskurina O.V., Nogovitsin I.V., et al. Formation of BiFeO₃ Nanoparticles Using Impinging Jets Microreactor. *Russian Journal of General Chemistry*, 2018, **88** (10), P. 2139–2143.
- [25] Gusarov V.V., Almjasheva O.V. *Nanomaterials: properties and promising applications*. Scientific world publishing house, Moscow, 2014, P. 378–403.
- [26] Martinson K.D., Kondrashkova I.S., Popkov V.I. Synthesis of EuFeO₃ nanocrystals by glycine-nitrate combustion method. *Russian Journal of Applied Chemistry*, 2017, **90** (8), P. 1214–1218.
- [27] Bachina A., Ivanov V.A., Popkov V.I. Peculiarities of LaFeO₃ nanocrystals formation via glycine-nitrate. *Nanosystems: Physics, Chemistry, Mathematics*, 2017, **8** (5), P. 647–653.
- [28] Popkov V.I., Almjasheva O.V., et al. Crystallization behaviour and morphological features of YFeO₃ nanocrystallites obtained by glycine-nitrate combustion. *Nanosystems: Physics, Chemistry, Mathematics*, 2015, **6** (6), P. 866–874.
- [29] Popkov V.I., Almjasheva O.V., et al. Effect of spatial constraints on the phase evolution of YFeO₃-based nanopowders under heat treatment of glycine-nitrate combustion products. *Ceramics International*, 2018, **44** (17), P. 20906–20912.
- [30] Lomanova N.A., Tomkovich M.V., Sokolov V.V., Gusarov V.V. Special Features of Formation of Nanocrystalline BiFeO₃ via the Glycine-Nitrate Combustion Method. *Russian Journal of General Chemistry*, 2016, **86** (10), P. 2256–2262.
- [31] Nguyen T.A., Nguyen T.Tr.L., et al. Optical and magnetic properties of HoFeO₃ nanocrystals prepared by a simple co-precipitation method using ethanol. *Journal of Alloys and Compounds*, 2020, **834**, P. 155098–155103.
- [32] Jiang L., Liu W., et al. Low-temperature combustion synthesis of nanocrystalline powders via a sol-gel method using glycine. *Ceramics International*, 2012, **38** (5), P. 3667–3672.
- [33] Luu M.D., Dao N.N., et al. Sol-gel synthesis of LaFeO₃ nanomaterials with perovskite structure. *Vietnam Journal of Chemistry*, 2014, **52** (1), P. 130–134.
- [34] JCPDS PCPDFWIN: A Windows Retrieval/Display Program for Accessing the ICDD PDF-2 File, ICDD, 1997.
- [35] Patterson A.L. The Scherrer formula for X-ray particle size determination. *Physics Review*, 1939, **56** (10), P. 978–982.
- [36] Nguyen T.A., Chau H.D., et al. Structural and magnetic properties of YFe_{1-x}Co_xO₃ (0.1 ≤ x ≤ 0.5) perovskite nanomaterials synthesized by co-precipitation method. *Nanosystems: Physics, Chemistry, Mathematics*, 2018, **9** (3), P. 424–429.
- [37] Nguyen T.A., Nguyen V.Y., et al. Synthesis and magnetic properties of PrFeO₃ nanopowders by the co-precipitation method using ethanol. *Nanosystems: Physics, Chemistry, Mathematics*, 2020, **11** (4), P. 468–473.
- [38] Ivanov V.K., Fedorov P.P., Baranchikov A.Y., Osiko V.V. Oriented aggregation of particles: 100 years of investigations of non-classical crystal growth. *Chemical Reviews*, 2014, **83** (12), P. 1204–1222.
- [39] Popkov V.I., Tugova E.A., Bachina A.K., Almyasheva O.V. The formation of nanocrystalline orthoferrites of rare-earth elements XFeO₃ (X = Y, La, Gd) via heat treatment of coprecipitated hydroxides. *Journal of General Chemistry*, 2017, **87** (11), P. 2516–2524.
- [40] Almjasheva O.V., Gusarov V.V. Metastable Clusters and Aggregative Nucleation Mechanism. *Nanosystems: Physics, Chemistry, Mathematics*, 2014, **5** (3), P. 405–416.
- [41] Almjasheva O.V., Fedorov B.A., Smirnov A.V., Gusarov V.V. Size, morphology and structure of the particles of zirconia nanopowder obtained under hydrothermal conditions. *Nanosystems: Physics, Chemistry, Mathematics*, 2010, **1** (1), P. 26–37.
- [42] Bhat M., Kaur B., et al. Swift heavy ion irradiation effects on structural and magnetic characteristics of RFeO₃ (R = Er, Ho and Y) crystals. *Nuclear Instruments and Methods in Physics Research B*, 2006, **243**, P. 134–142.
- [43] Nguyen T.A., Pham V., et al. Simple synthesis of NdFeO₃ nanoparticles by the so-precipitation method based on a study of thermal behaviors of Fe (III) and Nd (III) hydroxides. *Crystals*, 2020, **10** (3), P. 219–227.
- [44] Sasikala C., Durairaj N., et al. Transition metal titanium (Ti) doped LaFeO₃ nanoparticles for enhanced optical structure and magnetic properties. *Journal of Alloys and Compounds*, 2017, **712**, P. 870–877.